Published in final edited form as:
Biochemistry. 2013 June 25; 52(25): 4422–4432. doi:10.1021/bi301368f.

Structural Changes in the Hydrophobic Hinge Region Adversely Affect the Activity and Fidelity of the I260Q Mutator DNA Polymerase β

Chelsea L. Gridley[†,‡], **Sneha Rangarajan**[†,‡], **Susan Firbank**[§], **Shibani Dalal**[‖], **Joann B. Sweasy**[‖], and **Joachim Jaeger**[*,†,‡]

[†]Division of Genetics, Wadsworth Center, New York State Department of Health, New Scotland Avenue, Albany, New York 12208, United States

[‡]Department of Biomedical Sciences, School of Public Health, University at Albany, 1400 Washington Avenue, Albany, New York 12222, United States

[§]Institute for Cell and Molecular Biosciences, Newcastle University, Newcastle NE2 4HH, U.K.

[‖]Department of Therapeutic Radiology, Yale Cancer Center, Cedar Street, New Haven, Connecticut 06520, United States

Abstract

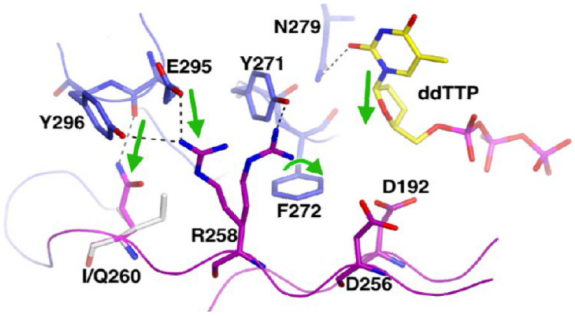

The I260Q variant of DNA polymerase β is an efficient mutator polymerase with fairly indiscriminate misincorporation activities opposite all template bases. Previous modeling studies have suggested that I260Q harbors structural variations in its hinge region. Here, we present the crystal structures of wild type and I260Q rat polymerase β in the presence and absence of substrates. Both the I260Q apoenzyme structure and the closed ternary complex with double-stranded DNA and ddTTP show ordered water molecules in the hydrophobic hinge near Gln260, whereas this is not the case in the wild type polymerase. Compared to wild type polymerase β ternary complexes, there are subtle movements around residues 260, 272, 295, and 296 in the mutant. The rearrangements in this region, coupled with side chain movements in the immediate neighborhood of the dNTP-binding pocket, namely, residues 258 and 272, provide an explanation for the altered activity and fidelity profiles observed in the I260Q mutator polymerase.

Faithful DNA replication and DNA repair are critical for the preservation of genomic integrity. The fidelity of a polymerase is defined as the ability to select the correct incoming

[*]Corresponding Author jj@wadsworth.org. Phone: (518) 408-2225. .

Notes The authors declare no competing financial interest.

dNTP over an incorrect one to form a Watson–Crick base pair for incorporation into the new strand of DNA. Repair polymerases are critical in preserving DNA integrity. DNA polymerase β (pol β) is a key player in the BER pathway and is responsible for repairing small stretches (one to six nucleotides) of damage in dsDNA. Pol β, which is highly conserved across eukaryotic organisms,[1] is the smallest and most thoroughly studied of the eukaryotic polymerases. The BER pathway removes damaged nucleotides and abasic sites that have been generated from reactive oxygen species (ROS) and other forms of cellular damage.[2] During BER, pol β recognizes and binds to 5′-deoxyribose phosphate (dRP) sites, left behind after the removal of damaged bases, where it removes the dRP moiety and fills the gap with a NTP complement to the template base.[3,4] As a contribution to its function in BER, pol β is a processive enzyme in short gap-filling synthesis on its preferred substrate, dsDNA with a gap of up to six nucleotides.[5,6] Because of its small size and relative ease of handling, pol β has been a model repair polymerase for studying the kinetics of nucleotide incorporation and the mechanism of DNA gap-filling repair processes: short-patch and long-patch BER.[7–9] However, if the polymerase becomes altered in a way that leads to the generation of subsequent mutations during DNA gap-filling synthesis and causes the accumulation of mutations in genomic DNA, then this can lead to abnormal manifestations, including human diseases such as cancer. In fact, several mutator mutants of pol β have been identified in a variety of human cancers,[10] indicative of a possible link between cancer and compromised repair polymerases.

A member of the X family of polymerases, pol β shares the characteristic “right-hand” polymerase domain (palm, fingers, and thumb) with many other eukaryotic polymerases.[11–13] Functionally, pol β is divided into two domains based on dRP lyase in the 8 kDa (N-terminal) domain and nucleotide transfer activity in the 31 kDa (C-terminal) domain. Pol β contains several sequence motifs that enhance the interactions of the enzyme with the gapped DNA substrate: two helix–hairpin–helix motifs in the 8 kDa and thumb subdomains[14,15] and carboxylate residues in the palm subdomain.[16] The palm subdomain of pol β houses the strictly conserved aspartate amino acids in the pol X family (Asp190, Asp192, and Asp256), which bind two metal ions. Like all other polymerases and many nucleases, pol β uses a two-metal ion mechanism for nucleotide transfer, which was first described in crystallographic detail in the exonuclease domain of *Escherichia coli* DNA polymerase I Klenow fragment.[17]

Many kinetic studies have characterized the numerous aspects of rat pol β activity: wild type, mutator mutants, and cancer-associated mutants, with a double-stranded or gapped DNA substrate, and incorporation rates for correct versus incorrect nucleotides.[18–23] The current literature highlights the altered *in vitro* and *in vivo* activity of pol β due to single-amino acid changes: I260Q misincorporates nucleotides because of a decreased level of dNTP discrimination during binding and extends beyond the mispaired primer terminus more often than the wild type;[24–26] D246V exhibits decreased fidelity compared to that of the wild type and lacks discrimination during dNTP binding;[27] M282L shows mutagenic properties both *in vitro* and *in vivo*.[28] Furthermore, three single-amino acid mutant forms of pol β, E295K, I260M, and P242R, have been linked to gastric cancer[29,30] and prostate cancer.[23,31] The vast majority of structural studies of pol β have been conducted with wild type polymerase, and thus far, structural information has only been obtained for two single-amino acid variants of pol β, M282L[22] and I260Q;[32] neither structure contains substrate. To improve our understanding of pol β structure–function relationships, high-resolution, complete structural characterizations of single-point mutator mutants of DNA polymerase β in the presence of substrate are required.

The I260Q variant of pol β is an active polymerase with strong mutator properties compared to the wild type: I260Q exhibits a 60-fold increase in reversion frequency in a Trp+

reversion assay *in vivo* and has an increase in the number of misincorporation events in a qualitative gap-filling synthesis *in vitro*.[33] I260Q exhibits a 19–23-fold decreased fidelity opposite template base A and a 16–30-fold decreased fidelity opposite template base C, compared to that of wild type pol β.[24] This residue maps to the hydrophobic hinge region at the boundary of the palm and fingers subdomains, an area known to influence the ability of pol β to discriminate during nucleotide binding.[24,33] The hydrophobic hinge (Ile174, Leu194, Thr196, Ile260, Tyr265, and Phe272)[33,34] of pol β and, in particular, the relative motion of the fingers subdomain about this hinge critically affect polymerase fidelity.[24] With residue 260 being 12–14 Å from the active site, the mutator activity of the I260Q pol β necessitates a thorough characterization of the structure of the mutant both locally near the mutation and globally to understand more comprehensively the mechanism of the mutator phenotype.

While numerous kinetic studies of pol β mutator mutants have revealed a link between residues distant from the active site,[26–28,35] such as those in the hydrophobic hinge,[24,28] and an increased rate of nucleotide misincorporation,[33] the structural information explaining possible long-range steric or electrostatic constraints is lacking. Modeling suggested that the more bulky glutamine residue would occupy more space in both apoenzyme and cocrystal structures than the native isoleucine residue.[28] Here, we present the first cocrystal structures of rat DNA pol β with Ile260 mutated to Gln in the presence and absence of substrates. The structures show how subtle changes in the hydrophobic hinge around Gln260 eventually alter the dNTP-binding pocket at the primer-binding site of pol β and provide a structural underpinning for how the activity and fidelity profiles of the I260Q mutator polymerase are altered.

EXPERIMENTAL PROCEDURES

Materials and Bacterial Strains

All chemicals were of the highest quality commercially available; dNTPs were purchased from GE Healthcare Life Sciences (Piscataway, NJ), and DNA oligomers were obtained from Integrated DNA Technologies (IDT DNA, Coralville, IA). Bacterial strain Rosetta2 DE3 with genotype F^- ompT $hsdS_B(r_B^- m_B^-)$ gal dcm (DE3) pRARE2 (Cam^R) was used for protein expression. The I260Q mutant was generated through Stratagene site-directed mutagenesis in a pET28a(+) vector (Novagen).[33]

Expression and Purification of Proteins

The full-length construct of rat pol β was expressed in Rosetta2 DE3 cells as previously described for similar pol β constructs.[36] The purification of wild type and I260Q pol β is based on a published purification protocol of Klenow fragment.[37,38] Briefly, the cells were resuspended in 25 mM HEPES (pH 7.0), 100 mM NaCl, and 5% glycerol with lysozyme in the presence of Protease Inhibitor Cocktail Tablets, EDTA-Free (Sigma-Aldrich), and sonicated (5 s pulse × 30 s rest) for 10 min while they were suspended in an ice/water bath, followed by ultracentrifugation. The protein mixture was filtered with 5 and 0.45 μm syringe filters before being loaded onto a HiTrap Heparin column and separated by a NaCl gradient [buffer A, 25 mM HEPES, 100 mM NaCl, and 5% glycerol (pH 7.0); buffer B, 25 mM HEPES and 2 M NaCl (pH 7.0)] using a liquid chromatography system (Aekta Prime, Amersham Biosciences). Fractions containing pol β were identified by electrophoresis on a 12.5% SDS–PAGE gel, pooled, diluted 1:5 with 25 mM HEPES and 25 mM NaCl (pH 7.0), loaded onto an SP Sepharose column, and again separated by a NaCl gradient [buffer C, 25 mM HEPES and 25 mM NaCl (pH 7.0); buffer B, 25 mM HEPES and 2 M NaCl (pH 7.0)]. Fractions containing pol β were identified again by electrophoresis via 12.5% SDS–PAGE, pooled, and concentrated to <5 mL before being loaded onto a gel filtration column (HiLoad

16/60 Superdex 75 prep grade, GE Healthcare Life Sciences). Protein was purified and buffer exchanged over the gel filtration column with buffers specific to the crystallization of the apoenzyme [20 mM $(NH_4)_2SO_4$ and 100 mM HEPES (pH 7.0)] or the dsDNA–pol β complex [100 mM MES, 10 mM $(NH_4)_2SO_4$, and 30 mM NaCl (pH 6.5)]. Following gel filtration of the polymerase, the protein was >95% pure as determined by SDS–PAGE and dynamic light scattering (data not shown). The concentration of the protein was calculated on the basis of an extinction coefficient of 23380 M^{-1} cm^{-1} and a molecular mass of 39 kDa.

In Vitro Primer Extension Assays

The substrates chosen in these primer extension assays are based on those used in our cocrystallization studies. The assay conditions were derived from previously published DNA pol β extension assays with slight modifications.[36] Briefly, the primer strand was labeled with a fluorescent probe at the 5′ end (5′-/6-FAM/ATG TGAG-3′), which when annealed to the template strand (5′-TAC GTC GCG ACT GCT CAC AT-3′) created a 7 bp duplex (underlined bases) with a 13-nucleotide 5′ overhang (Integrated DNA Technologies). The primer and template were annealed in 50 mM Tris (pH 8.0) and 250 mM NaCl; annealing was verified with dynamic light scattering (data not shown). Enzyme:DNA ratios ranged from 50:1 to 10:1, where the DNA concentration was 45 nM and the enzyme concentration was 450 nM. The assay was performed at 37 °C in 20 mM Tris (pH 8.0), 60 mM NaCl, 10% glycerol, and 1 mM dithiothreitol (final concentrations). The DNA and protein were mixed with reaction buffer and preincubated if indicated, and the reaction was initiated via the addition of dNTPs (final concentration of 50 μM) and $MgCl_2$ (final concentration of 10 mM). After 5 min, the reaction was quenched with an equal volume of TBE-urea sample buffer, 89 mM Tris, 89 mM boric acid, 2 mM EDTA (pH 8.0), 12% Ficoll, 0.01% bromophenol blue, 0.02% xylene cyanol FF, and 7 M urea (Bio-Rad Laboratories, Inc.), and samples were heated to 95 °C for 5 min before being separated on a 15% TBE-urea denaturing PAGE gel. Gels were then visualized on a Typhoon Imager (GE Healthcare Life Sciences) for the detection of fluorescent bands indicating extended versus unextended primer.

In Vitro Misincorporation Assays

To verify the mutator phenotype of pol β I260Q, we modified the primer extension assay to determine the misincorporation and mispair extension activity of the mutant versus wild type. Using the same dsDNA substrate described above that was annealed as described above, we omitted either the first or the second nucleotide for incorporation from the dNTP mixture used to initiate the reaction. Accordingly, either dCTP or dATP was omitted from the reaction. The enzyme:DNA ratio was 10:1, with 450 nM wild type or I260Q pol β and 45 nM DNA. The enzyme and DNA were mixed and preincubated for 5 min, after which the dNTPs (final concentration of 50 μM) and $MgCl_2$ (final concentration of 10 mM) were added to start the reaction. The assay conditions were the same as in the primer extension assay. For comparison, we included a positive and negative control for each protein sample at each time point: the positive control contained all four dNTPs, indicted by “0” missing nucleotides below the respective lanes, and the negative control lacked $MgCl_2$ and all dNTPs, indicated by “4” missing nucleotides below the respective lanes. At 2, 10, and 30 min, 5 μL aliquots from each reaction mixture were quenched with the TBE-urea buffer detailed above, heated to 95 °C, separated on a 15% TBE-urea denaturing PAGE gel, and visualized on a Typhoon Imager (GE Healthcare Life Sciences).

Crystallization of the Pol β Apoenzyme

Pol β was typically concentrated to ~20 mg/mL before the crystallization trials were set up. The protein to be crystallized in the apoenzyme form was buffer exchanged into 10 mM

$(NH_4)_2SO_4$ and 100 mM HEPES (pH 7.0) and crystallized by vapor diffusion in a sitting drop. The protein and well solution were mixed in equal volumes for crystallization. The initial protein concentration was 10 mg/mL using a well solution containing 9–12% PEG3350 and 90–120 mM MES (pH 7.0) (initial concentrations). Crystals of the apoenzyme form were cryoprotected with 20–22% 2-methyl-2,4-pentanediol (MPD) prior to being flash-cooled in liquid nitrogen.

Crystallization of Pol β Ternary Complexes

The protein to be cocrystallized with DNA and ddTTP was buffer exchanged into 100 mM MES (pH 6.5), 30 mM NaCl, and 10 mM $(NH_4)_2SO_4$. Pol β wild type and mutant cocrystals contained primer (5′-ATG TGA G-3′) and template (5′-CAA ACT CAC AT-3′) (Integrated DNA Technologies) resuspended in water and annealed in a 1:1 ratio in 20 mM $MgSO_4$ (90 °C for 2 min, 70 °C for 2 min, and 55 °C for 1 min and then cooled to 4 °C at a rate of 0.5 °C/min) in a DNA Dyad Peltier Thermal Cycler (MJ Research, Inc.). Mixtures of 230 μM protein, 290 μM DNA, and 2.5 mM ddTTP were aliquoted into 96-well MRC-2 crystallization plates (Hampton Research) for sitting drop screens and combined in a 1:1 ratio with reservoir solution (1.5 μL each). Crystals were grown over a reservoir of 120–200 mM NaCl, 6–14% PEG3350, 3% glycerol, and 50 mM cacodylate (pH 6.5). Prior to the crystals being flash-frozen in liquid nitrogen, a cryoprotectant mixture of 15% glycerol, 8 mM ddTTP, and well solution corresponding to the mother liquor was soaked into the drop. The excess ddTTP was added to maintain the high occupancy for the active site ligands. Cocrystals with the same DNA substrate and mismatched dNTPs were not single and diffracted very poorly.

Data Collection and Structure Refinement

X-ray intensity data were collected at beamlines X4C, X29, and X25 at the National Synchrotron Light Source (NSLS) at Brookhaven National Laboratory (Upton, NY). Data integration and reduction were performed using either HKL2000[39] or iMosflm version 1.5.0.[40] Structure determination was initiated using PHENIX version 1.7.4.[41] The structures of the $P2_1$ monoclinic apoenzyme pol β crystal forms were determined by molecular replacement using PHASER[42] with a composite model of apoenzyme pol β (X-ray structure of the 31 kDa domain and NMR structure of the 8 kDa domain) followed by rigid body refinement, full atomic refinement interspersed with manual rebuilding in COOT.[43] The ternary complex, in unrelated monoclinic space group $P2_1$, was determined by molecular replacement using an arrested rat pol β ternary complex [Protein Data Bank (PDB) entry 1HUO]. Subsequent refinement and model building were conducted again using PHENIX and COOT. Final structures were analyzed and verified using COOT, LSQMAN,[44] MolProbity,[45] and PyMol.[46]

RESULTS

Pol β I260Q Polymerase Activity on the Short Cocrystallization Oligonucleotides

The strong mutator activity of I260Q pol β has been characterized on an assortment of DNA substrates, double-stranded and 1 and 5 bp-gapped DNA, with varying primer and template sequences.[24,26,33,47] As the mutator polymerase crystallized and diffracted well when it was complexed with our short dsDNA complex, ddTTP, and sodium, we determined the activity of pol β on these cocrystallization oligonucleotides, with slight modifications. A simple fluorescent primer extension assay was designed essentially on the basis of the short cocrystallization oligomers (primer + template 5′-6-FAM-ATG TGA G-3′ + 5′-CAA ACT CAC AT-3′). The 5′ overhang on the template DNA was extended such that full-length products, at 20 nucleotides, could be easily distinguished from the original primer, at 7 nucleotides, with TBE-urea denaturing PAGE (see Experimental Procedures). Wild type pol

β served as a positive control as its activity has been well characterized for a wide range of substrates and conditions,[27,28] and a polymerase/DNA mixture without dNTPs or $MgCl_2$ served as a negative control (Figure 1A, lane 1). Figure 1A verifies that both wild type and I260Q pol β are able to extend the dsDNA substrate in the presence (lanes 3–5 and 7–9) and absence (lanes 2 and 6) of pol β–DNA preincubation. Preincubation allows time for the polymerase to form a stable complex with the DNA substrate. Without preincubation, I260Q pol β exhibits a slight increase in the extent of primer extension compared to that of the wild type after reaction for 5 min, as determined by the fluorescence intensity of the fully extended primer 20 nucleotides in length (Figure 1A, lanes 5 and 7). If the reaction mixtures are preincubated for at least 20 min, this difference in primer extension between wild type and I260Q pol β disappears, which is in line with the kinetic data for correct insertion published by Roettger. Of note is an intermediate-sized band observed in the extension and misincorporation assays, likely indicative of a stalled polymerase. With pol β preferring to repair short patches of nucleotides and given the length of the chosen 5′ overhang in the template strand, some stalling is observed (Figure 1A).

To determine the ability of I260Q pol β to misincorporate nucleotides on the same recessed DNA substrate, we systematically omitted from the reaction mix the first or second nucleotide required for faithful incorporation opposite template 3′-TA CAC TCG TCA GCG CTG CAT-5′, dCTP or dATP, respectively. For primer extension in the absence of dATP, the correct nucleotide, dCTP, is available for the first round of incorporation, but to proceed, the polymerase must then add an incorrect nucleotide. Wild type pol β shows little to no activity in this misincorporation assay until after 30 min, at which point only minimal levels of extended primer are detected (Figure 1B, lanes 15 and 16). The amount of extended primer under these conditions indicates that I260Q is able to misincorporate and extend mispaired dNTPs to a greater extent than the wild type (Figure 1B, lanes 7 and 8 and lanes 11 and 12). The observed increase in the extended primer with I260Q indicates that this mutator variant of pol β is more likely to allow a misincorporation event and create more extended primer product than the wild type under these conditions. Overall, the dsDNA used for our cocrystallization trials is a suitable substrate for wild type and I260Q pol β; furthermore, I260Q exhibits a mutator phenotype on this substrate, whereas the wild type does not.

Apoenzyme Structure of Wild Type and I260Q DNA Polymerase β

To identify structural differences between I260Q and the wild type in the absence of substrate, we crystallized each polymerase without DNA or dNTP. The wild type polymerase and I260Q mutant crystallized in the same space group, $P2_1$, with comparable unit cell dimensions (Table 1). Data were collected at resolutions of 2.4 and 2.2 Å for the wild type and I260Q, respectively. Each crystal form contains two molecules per asymmetric unit (ASU). The ASU of I260Q apoenzyme pol β is shown in Figure 2A. The two molecules in the ASU for apo wild type and apo I260Q superimpose with respective overall root-mean-square deviations (rmsds) of 1.058 and 1.109 Å, respectively (Figure 2B). For the sake of clarity, the wild type or I260Q apoenzyme pol β molecule with the best corresponding electron density and lowest average temperature factors is shown, unless otherwise stated.

Both wild type and I260Q apo polymerase structures are full-length and adopt a wide-open conformation of the polymerase and lyase domains (Figure 2B), somewhat reminiscent of but not identical or isomorphous to that of rat apo pol β (PDB entry 1BPD).[16,32,48] The greatest distance between the 8 kDa subdomain and the tip of the fingers subdomain, i.e., Asn24 and Thr304, is ~50 Å in both of our apo polymerases. In the hydrophobic hinge region of wild type and I260Q apo pol β, three residues are in the proximity of the side chain

at position 260: Tyr296, Arg258, and Leu194 as indicated in Figure 2B. The residues in this hinge must allow for the closure of the fingers subdomain over the palm during catalysis.

The I260Q mutation inserts a polar side chain into a hydrophobic region and causes a cascade of subtle changes, which contribute to the altered fidelity of this pol β variant. The flexibility of the hinge region is decreased in I260Q as seen from a comparison of normalized atomic temperature factors in wild type pol β and the variant. The analysis shows that unlike in the wild type apo polymerase structure prominent hinge residues in I260Q pol β have normalized B values consistently lower than the molecular average. The distance between residue 260 and Tyr296 or Leu194 varies only slightly (±0.4 Å) between wild type and I260Q apo structures. Arg258 is known to form a weak salt bridge with Asp192 in the open polymerase conformation.[16] The conformation and orientation of Arg258, relative to the catalytic Asp192 residue, vary between our wild type and I260Q apo polymerases: the Arg258 side chain is more proximal to Asp192 (2.7 Å) in the mutant than in the wild type (3.5 Å). We observe the coordination of several well-defined water molecules in the I260Q apoenzyme structure (Figure 2C), which are not evident in the sufficiently detailed electron density maps of wild type pol β (Figure 2D). The presence of water molecules (Figure 2C and Table 1) in this normally hydrophobic hinge region of I260Q is a direct result of the polar glutamine side chain and the corresponding changes around position 260. The glutamine at position 260 in the pol β variant is more bulky and occupies more space within the hydrophobic hinge than the native isoleucine.

Structure of the I260Q Pol β Ternary Complex

The I260Q mutator pol β variant was crystallized as a ternary complex with a recessed primer (5′-ATG TGA G-3′) and template (5′-CAA ACT CAC AT-3′), ddTTP, and Na^+ (Figure 3A). The template DNA was limited to a 4-nucleotide 5′ overhang to prevent unwanted disorder during nucleation or weak crystal contacts with symmetry-related polymerase molecules. The structure of the I260Q pol β ternary complex was determined at 2.7 Å, belonging to monoclinic space group $P2_1$ with two molecules in the ASU (Table 1). The two molecules in the I260Q ternary complex ASU match closely, and palm subdomains superimpose with an rmsd of Cα positions of 0.415 Å (overall rmsd of 0.861 Å). An arrested ternary complex of wild type rat pol β, PDB entry 1HUO,[49] with unit cell dimensions and a crystal packing arrangement closely related to those of our ternary I260Q complex, was used as a trial structure for molecular replacement.

Molecular replacement using PDB entry 1HUO as a reference model for the I260Q ternary complex produced a single solution with an initial R factor of 0.37 at 2.8 Å resolution. The 1HUO structure of wild type pol β represents a coordinated rat pol β·dsDNA·[Cr(III)-dTMPPCP] complex.[49] In that structure, the trapped form of dTMPPCP allowed the crystallization of the polymerase in the presence of a free hydroxyl group on the primer 3′ terminus, for the first time capturing the fully functional intermediate state. A related ternary structure of wild type pol β, PDB entry 2FMP, is a human pol β·1-nucleotide gapped DNA·[Mg^{2+}-ddCTP] complex with Na^+ coordinated as the catalytic metal.[50] While the equivalent atoms of the incoming nucleotides (ddTTP in I260Q ternary and ddCTP in 2FMP) and metal ions A and B are in superb agreement and superimpose with an rmsd of 0.398 Å, the overall structures superimpose poorly, with rmsds of 2.622–3.053 Å, for the two molecules of I260Q ternary pol β in the ASU. Although the crystallization conditions of the rat and human ternary pol β complexes included different metal ions (I260Q, Na^+; 1HUO, Cr^{3+}; 2FMP, Na^+/Mg^{2+}), there is generally excellent agreement in the residues lining the dNTP-binding pocket. Therefore, the size, charge, and chemical nature of these cations do not affect the arrangement of active site residues and with the screening by surrounding residues will not affect the side chain rearrangements near the site of the mutation in the I260Q variant. However, the differences between rat and human pol β, 14 amino acid changes, and

the divergent DNA substrates, dsDNA in I260Q ternary and 1HUO, and single-gap DNA in 2FMP, prompted us to conduct a more detailed analysis of the site of mutation and the active site center between rat I260Q pol β and nearly isomorphous wild type (1HUO) ternary complexes.

Globally, the I260Q mutant is similar to 1HUO in terms of the overall architecture and secondary structure elements (Figure 3B). For the sake of clarity, the molecule with the best corresponding electron density and lowest average temperature factors will be used in our comparisons and discussions, for ternary pol β, I260Q, and wild type. The α-carbon atoms of 303 residues in I260Q and 1HUO can be superimposed with an rmsd of 1.071 Å. The α-carbon atoms of the N-terminal domains (residues 10–91) and those of the palm subdomains (residues 150–261) agree well with rmsds of 0.56 and 0.45 Å, respectively. Subtle differences were observed in the fingers subdomain (residues 262–334, rmsd of 0.80 Å) and palm residues adjacent to the site of mutation (as discussed below).

Because residue 260 is more than 16 Å from metal B in the active site, any effect on polymerase activity must be long-range and occur indirectly via neighboring residues. The amino acids in the vicinity of residue 260 interact with Ile and Gln differently in the wild type and the I260Q ternary complex of pol β. Consequently, the flexibility of the hinge region is decreased as seen from a comparison of normalized atomic temperature factors of residues in this region. The difference in resolution between the wild type and I260Q diffraction data prevents a reliable determination of F_{000} and precludes a meaningful analysis of the Wilson scale (data not shown). However, in line with the observations for the apo polymerase structures, the hinge residues in the ternary complex of I260Q pol β consistently show up to 40% lower than average atomic B values, whereas the wild type ternary complex (1HUO) has temperature factors near or above the molecular average (data not shown). The stabilization of hinge residues is a result of, in part, the formation of a hydrogen bond between the amide side chain of Gln260 and the backbone of Glu295 (Figure 3C,D). This interaction is not observed in the wild type ternary pol β. This hydrogen bond between Gln260 and Glu295 stabilizes the ternary complex and secures the observed orientation of the glutamine side chain (second most common rotamer, for which χ_1 = −174°). Residues on either side of the hydrophobic hinge, Tyr296 and Arg258, highlight the increased number of constraints in the I260Q variant as compared to a more flexible hydrophobic hinge in the wild type.

The effect of substrate binding on the residues of the hydrophobic hinge can be seen by comparing the apoenzyme and ternary complex of I260Q (Figure 3C). In the apo form, Arg258 and Asp192 show significant interactions. In the DNA cocrystals, however, Arg258 moves away from Asp192 and is now observed in two distinct conformations pointing toward the fingers domain. Through the presence of polar and charged residues in the mutator mutant, the more prominent of the two conformations of Arg258 [on the left at 70% occupancy (Figure 3D)] is within 3.8 Å of Gln260, whereas an alternate, less frequent conformation of Arg258 [to the right at 30% occupancy (Figure 3D)] is 6.3 Å from Gln260. Furthermore, in the I260Q ternary complex, Arg258 in its predominant conformation interacts strongly with the side chain of Try296. By contrast, the length of this salt bridge changes by more than 1 Å in the wild type complex (1HUO), thereby weakening the interactions between the palm (Arg258) and fingers (Tyr296) (see Figure 3D). The second conformation of Arg258 in the I260Q ternary complex is oriented toward the active site, but not as much as in apo pol β (Figure 3C). Thus, the switching of Arg258 represents a direct link between the presence (or absence) of a polar side chain at position 260 and the polymerase active site, namely residue Asp192, which critically affects activity. Significant side chain movements are also observed in both wild type and I260Q ternary complexes

near I/Q260 involving Arg258 and Phe272 (Figure 3D). These two residues are immediately adjacent to the active site influencing Asp192 and its role in the catalytic cycle.

dNTP–metal B binding causes the fingers subdomain to close upon the active site.[51] This large conformational change is accompanied by more subtle side chain rearrangements creating the appropriate geometry in the active site. In the wild type (1HUO), Phe272 has rotated down and interrupted the salt bridge between Arg258 and Asp192, forcing these residues 8.4 Å apart (Figure 3D). This movement allows Asp192 to participate exclusively in the critical ion-mediated interactions with the two other catalytic aspartates (Asp190 and Asp256). The mutator ternary complex of I260Q pol β shows the aromatic ring of Phe272 tilted (χ_2 = 13°) toward Asp192, whereas in the wild type, this aromatic ring (χ_2 = 109°) is pointing away from Asp192 (Figure 3D). The side chain arrangement of Phe272 is important because of its backbone linkage to Tyr271, a residue that directly interacts with the primer terminus via hydrogen bonding with the minor groove edge of the primer DNA.[52]

Finally, we compared the interactions among the ddTTP, Asn279, and nearby residues in the active site. The structure of the wild type pol β ternary complex reveals that Nδ2 of Asn279 forms a single hydrogen bond with O2 in the base of the incoming ddCTP.[53] In the mutator pol β variant, I260Q, we observed a shift of Asn279, by 1.0 Å, away from the ddTTP ribose moiety compared to that in the wild type. This small change leaves the dNTP-binding residue, Asp279, 3.6 Å from the incoming nucleotide. The relaxed geometric constraints at the metal-binding site (Asp192), primer base positioning (Phe272), and dNTP binding (Asp279) explain the mutator activity of I260Q pol β, detailed in the Discussion.

DISCUSSION

The fidelity of DNA replication and repair is dependent on the ability of the DNA polymerase to select and incorporate the correct dNTP to complement the template strand among a pool of dNTP substrates. Despite the lack of an endonuclease domain, or proofreading activity, pol β creates only one error in every 5000 incorporation events *in vivo*.[54] As a repair polymerase, the DNA repair fidelity of pol β is crucial for maintaining genomic integrity. A single-point mutation, I260Q, alters activity and fidelity compared to those of the wild type, while being located in a region 12–14 Å from the polymerase catalytic center. I260Q pol β shows an increased affinity for mismatched dNTP[24,25] and, furthermore, an increased probability of incorporating the incorrect nucleotide[33] and extending beyond the mispairs.[25] In fact, in a Trp+ reversion assay, I260Q exhibits a 14.5-fold increase in mispair extension efficiency compared to that of the wild type.[23] Structural comparisons between the wild type and I260Q polymerases, in the absence of substrate and in their respective ternary complexes, has allowed us to gain structural insights and an improved understanding of the altered phenotype of this mutator mutant.

Overall, the wild type and I260Q apoenzyme structures differ only slightly in their overall conformations (Figure 2B), which is in good agreement with their similar secondary structure content as determined by circular dichroism.[33] The two pol β polymerases also exhibit comparable rates of nucleotide incorporation and catalytic efficiency in an *in vitro* gap filling assay with all four nucleotides,[33] in stopped-flow fluorescence assays with matched incoming nucleotides,[26] and in our *in vitro* primer extension assay with all four nucleotides (Figure 1A). It is important to note that on correct insertion wild type and I260Q pol β show no difference in incorporation efficiency on our 3′ recessed substrate if the reaction mixtures are preincubated for 30 min. This nicely confirms the data with a gapped DNA substrate (1-nucleotide gap) published by Roettger et al., who found the differences in enzyme efficiencies between the wild type and mutant polymerase to be negligible: k_{pol}/

$K_{d,app}^{(C:dGTP)}$ = 9.7 μM^{-1} s^{-1} for the wild type and 15 μM^{-1} s^{-1} for I260Q, and $k_{pol}/K_{d,app}^{(T:dATP)}$ = 6.3 μM^{-1} s^{-1} for the wild type and 6.2 μM^{-1} s^{-1} for I260Q.[26]

The catalytic efficiency of mispair extension was determined for I260Q and the wild type on a 5 bp gapped DNA substrate in the presence of a mispaired primer terminus (A:dATP): I260Q bound the dNTP substrate more tightly (K_d = 0.6 μM) and catalyzed its incorporation (k_{pol}/K_d = 4.0 × 10^4 M^{-1} s^{-1}) more efficiently than the wild type (K_d = 13.8 μM; k_{pol}/K_d = 2.75 × 10^3 M^{-1} s^{-1}).[25] Similarly, Roettger and co-workers used stopped-flow and quench-flow assays to measure the kinetics of matched versus mismatched dNTP incorporation on a 1-nucleotide gapped DNA substrate. In the case of a T:dGTP mismatch, I260Q bound the mismatched nucleotide more tightly (K_d = 49 ± 3 μM) and incorporated it more efficiently (k_{pol}/K_d = 2.8 × 10^{-4} M^{-1} s^{-1}) than the wild type (K_d = 489 ± 26 μM; k_{pol}/K_d = 1.2 × 10^{-5} M^{-1} s^{-1}) (similar values were observed for the C:dATP mismatch).[26] These findings indicate that the I260Q mutator polymerase has lost some of its ability to discriminate correct versus incorrect dNTP, at the level of ground-state binding, in the presence of mispaired primer terminus, as compared to that of the wild type.[25] Taken together, these results provide evidence to support the proposed mutator phenotype of I260Q in the presence of various DNA substrates and opposite all template bases. Because well-diffracting crystals of I260Q pol β in complex with dsDNA and ddTTP could be obtained readily, the basic activity and mutator phenotype of this variant was tested on a 3′ recessed substrate that was used in the crystallographic studies. We found that I260Q is a strong mutator polymerase on the gapped DNA substrates[25,26] and exhibits a tendency to misincorporate and extend mispairs on our 3′ recessed substrate (Figure 1B).

Steady-state kinetic studies of pol β reveal a significant difference between the wild type and I260Q in terms of dNTP-induced conformational changes. With stopped-flow fluorescence, Roettger et al. concluded that while wild type and I260Q pol β both exhibit fast conformational changes in the presence of matched and mismatched nucleotides, I260Q creates a more stable mismatch ternary complex than the wild type.[26] Additionally, the wild type polymerase is quick to release the mismatch (K_d values of 489 ± 26 μM for T:G and 227 ± 22 μM for C:A), yet the I260Q mutant polymerase appears to stabilize the mismatch (K_d values of 49 ± 3 μM for T:G and 45 ± 3 μM for C:A), which may further explain the enhanced misincorporation properties of this polymerase.[26] An early hypothesis suggested that the I260Q mutation might translate into altered binding of the polymerase to the DNA substrate and the accommodation of an incorrect nucleotide substrate in the active site of the mutant polymerase.[33] Of particular interest though are the mechanisms by which the I260Q mutation decreases the fidelity of the polymerase. The underlying structural reasons for the altered fidelity appear to be twofold: (i) hydrogen bonds in the hydrophobic hinge and (ii) internal side chain rearrangements in or near the dNTP-binding pocket of I260Q.

First, our apo crystal form of I260Q pol β not previously described shows the coordination of water molecules in the hydrophobic hinge region (Figure 2C). Unlike the wild type apo polymerase, where the hydrophobic hinge is free of solvent molecules, the ordered waters and nearby structural changes are due to the more polar nature around the site of mutation (Gln260). Some or all of the water molecules may need to be expelled before the I260Q fingers subdomain can close around the substrate, which may slow the process or make it less energetically favorable. One of the critical conformational steps in catalysis involves the rotation of the pol β fingers subdomain toward the palm subdomain, induced by dNTP–metal ion binding in the active site.[50] In pol β, this movement is intimately linked to the hydrophobic hinge, of which Ile260 is an integral residue.[24] The presence of direct or water-mediated hydrogen bonds in the hinge region could also influence the equilibrium between the open and closed forms of pol β. We speculate that strengthening or favoring the closed

conformation could in turn improve dNTP binding, causing a significant decrease in K_d as observed in the kinetic studies.[25,26,33]

Second, the consequences of the I260Q mutation become more evident when the enzyme is cocrystallized and forms a complex with DNA and ddTTP. Aside from exterior changes on the surface of the hinge region, there are some significant differences in the interior, namely the way in which Ile260 and Gln260 interact with Arg258 and the carbonyl oxygen of Glu295. The interaction with Glu295 on the β-hairpin after helix N should further stabilize the closed conformation in the I260Q mutant. Furthermore, in wild type and I260Q pol β apoenzymes, Arg258 interacts closely with Tyr271, Phe272, and Asp192. When DNA or dNTP binds, Arg258 becomes repositioned closer to Gln260, prompting Asp192 to participate in metal coordination at the active site. Concurrently, Phe272 rotates to the space just above and between Arg258 and Asp192 as Tyr271 forms hydrogen bonds with the primer terminus. In the apoenzyme structures of the wild type and I260Q, Ile/Gln260 is distant from Arg258, which is found in the proximity of Phe272. In the cocrystal, however, Gln260 is in a position to predominantly interact with Arg258 conformer 1 (70% occupancy), and consequently, Arg258 and Phe272 are now separated by more than 5 Å, leaving Tyr271 in a suboptimal position for binding the primer terminus.

Furthermore, Phe272 now adopts a different side chain orientation ($\Delta\chi_2 \sim 70°$) compared to that of the wild type ternary complex (Figure 3D). Ile260, because of its hydrophobic nature, is unable to create this strong “cascade” effect, leaving Arg258 and Phe272 closer together, while Tyr271 remains in a position to interact with the primer terminus for efficient nucleotide incorporation. In the I260Q mutator mutant, it is the altered positioning of three crucial substrate-binding residues, Arg258, Tyr271, and Phe272, that slightly increases the volume of the dNTP-binding pocket around the ribose moiety, thereby presumably allowing the mutant to accommodate mismatched nucleotides more readily than the wild type. We suspect that the increased volume, the lowered level of ground-state binding for both mismatched and cognate dNTPs, and the stabilized closed conformation allow for a more efficient nucleotidyl transfer in I260Q pol β than in the parent enzyme.

To summarize, our structures, in their apoenzyme forms and in complex with a primer/template, ddTTP, and metal ions, provide a compelling structural foundation for the argument that three subtle differences in the hinge region around residues Ile/Gln260, Arg258, Glu295, and Tyr296 coupled with side chain rearrangements (mainly residues Arg258 and Phe272) immediately adjacent to the dNTP-binding pocket are sufficient to alter the activity and fidelity profile of wild type pol β to that observed in the I260Q mutator polymerase. To further improve our understanding of the mechanism of the mutator phenotype of I260Q pol β, structural studies with mismatched incoming dNTPs and gapped DNA would be useful, but so far, such cocrystals proved to be difficult to obtain with the rat enzyme.

Acknowledgments

Access to New York Structural Biology beamline X4C at the NSLS and on-site experimental and computational support by J. Schwanof and R. Abramowitz are gratefully acknowledged. Furthermore, we thank A. Heroux, H. Robinson, and other beamline staff at PXRR X25 and X29 at NSLS for access and on-site support with data collection, reduction, and back-up. Other support by the Macromolecular Crystallography and Biochemistry Instrumentation core facilities at the Wadsworth Center and support by Health Research Inc. are gratefully acknowledged.

Funding This work was supported in part by National Cancer Institute Grant 5R01 CA080830-13 to J.B.S. and J.J.

ABBREVIATIONS

pol β	DNA polymerase β
dNTP	2′-deoxyribonucleoside 5′-triphosphate
dsDNA	double-stranded DNA
BER	base excision repair
NER	nucleotide excision repair
dRP	5′-deoxyribose phosphate
HEPES	4-(2-hydroxyethyl)-1-piperazineethanesulfonic acid
EDTA	ethylenediaminetetraacetic acid
SDS–PAGE	sodium dodecyl sulfate–polyacrylamide gel electrophoresis
rmsd	root-mean-square deviation

REFERENCES

(1). Uchiyama Y, Takeuchi R, Kodera H, Sakaguchi K. Distribution and roles of X-family DNA polymerases in eukaryotes. Biochimie. 2009; 91:165–170. [PubMed: 18706967]

(2). Maynard S, Schurman SH, Harboe C, Souza-Pinto NC, Borh VA. Base excision repair of oxidative DNA damage and association with cancer and aging. Carcinogenesis. 2009; 30:2–10. [PubMed: 18978338]

(3). Matsumoto Y, Kim K. Excision of deoxyribose phosphate residues by DNA polymerase β during DNA repair. Science. 1995; 269:699–702. [PubMed: 7624801]

(4). Wilson S. Mammalian base excision repair and DNA polymerase β. Mutat. Res. 1998; 407:203–215. [PubMed: 9653447]

(5). Singhal RK, Wilson SH. Short Gap-filling Synthesis by DNA Polymerase β Is Processive. J. Biol. Chem. 1993; 268:15906–15911. [PubMed: 8340415]

(6). Prasad R, Beard WA, Wilson SH. Studies of Gapped DNA Substrate Binding by Mammalian DNA Polymerase β. J. Biol. Chem. 1994; 269:18096–18101. [PubMed: 8027071]

(7). Fortini P, Pascucci B, Parlanti E, Sobol RW, Wilson SH, Dogliotti E. Different DNA polymerases are involved in short- and long-patch base excision repair in mammalian cells. Biochemistry. 1998; 37:3575–3580. [PubMed: 9530283]

(8). Klungland A, Lindhal T. Second pathway for completion of human DNA base excision-repair: Reconstitution with purified proteins and requirement for DNase IV (FEN1). EMBO J. 1997; 16:3341–3348. [PubMed: 9214649]

(9). Podlutsky AJ, Dianova II, Wilson SH, Bohr VA, Dianov GL. DNA synthesis and dRPase activity of polymerase β are both essential for single-nucleotide patch base excision repair in mammalian cell extracts. Biochemistry. 2001; 40:809–813. [PubMed: 11170398]

(10). Starcevic D, Dalal S, Sweasy JB. Is There a Link Between DNA Polymerase β and Cancer? Cell Cycle. 2004; 3:998–1001. [PubMed: 15280658]

(11). Joyce CM, Steitz TA. Polymerase Structures and Functions: Variations on a Theme? J. Bacteriol. 1995; 177:6321–6329. [PubMed: 7592405]

(12). Jaeger J, Pata JD. Getting a grip: Polymerases and their substrate complexes. Curr. Opin. Struct. Biol. 1999; 9:21–28. [PubMed: 10047577]

(13). Steitz TA, Smerdon SJ, Jaeger J, Joyce CM. A Unified Polymerase Mechanism for Nonhomologous DNA and RNA Polymerases. Science. 1994; 266:2022–2025. [PubMed: 7528445]

(14). Pelletier H, Sawaya MR. Characterization of the Metal Ion Binding Helix-Hairpin-Helix Motifs in Human DNA Polymerase β by X-ray Structural Analysis. Biochemistry. 1996; 35:12778–12787. [PubMed: 8841120]

(15). Mullen GP, Wilson SH. DNA polymerase β in abasic site repair: A structurally conserved helix-hairpin-helix motif in lesion detection by base excision repair enzymes. Biochemistry. 1997; 36:4713–4717. [PubMed: 9125491]

(16). Sawaya MR, Prasad R, Wilson SH, Kraut J, Pelletier H. Crystal structures of human DNA polymerase β complexed with gapped and nicked DNA: Evidence for an induced fit mechanism. Biochemistry. 1997; 36:11205–11215. [PubMed: 9287163]

(17). Beese LS, Steitz TA. Structural basis for the 3′-5′ exonuclease activity of *Escherichia coli* DNA polymerase I: A two metal ion mechanism. EMBO J. 1991; 10:25–33. [PubMed: 1989886]

(18). Werneburg BG, Ahn J, Zhong X, Hondal RJ, Kraynov VS, Tsai MD. DNA polymerase β: Pre-steady-state kinetic analysis and roles of arginine-283 in catalysis and fidelity. Biochemistry. 1996; 35:7041–7050. [PubMed: 8679529]

(19). Kraynov VS, Showalter AK, Liu J, Zhong X, Tsai MD. DNA Polymerase β: Contributions of Template-Positioning and dNTP Triphosphate-Binding Residues to Catalysis and Fidelity. Biochemistry. 2000; 39:16008–16015. [PubMed: 11123928]

(20). Opresko PL, Sweasy JB, Eckert KA. The Mutator Form of Polymerase β with Amino Acid Substitution at Tyrosine 265 in the Hinge Region Displays an Increase in both Base Substitution and Frame Shift Errors. Biochemistry. 1998; 37:2111–2119. [PubMed: 9485358]

(21). Li S-X, Vaccaro JA, Sweasy JB. Involvement of Phenylalanine 272 of DNA Polymerase β in Discriminating between Correct and Incorrect Deoxynucleoside Triphosphates. Biochemistry. 1999; 38:4800–4808. [PubMed: 10200168]

(22). Shah AM, Conn DA, Li SX, Capaldi A, Jager J, Sweasy JB. A DNA polymerase β mutator mutant with reduced nucleotide discrimination and increase protein stability. Biochemistry. 2001; 40:11372–11381. [PubMed: 11560485]

(23). Dalal S, Hile S, Eckert KA, Sun K.-w. Starcevic D, Sweasy JB. Prostate-Cancer-Associated I260M Variant of DNA Polymerase β Is a Sequence-Specific Mutator. Biochemistry. 2005; 44:15664–15673. [PubMed: 16313169]

(24). Starcevic D, Dalal S, Jaeger J, Sweasy JB. The Hydrophobic Hinge Region of Rat DNA Polymerase β Is Critical for Substrate Binding Pocket Geometry. J. Biol. Chem. 2005; 280:28388–28393. [PubMed: 15901725]

(25). Dalal S, Starcevic D, Jaeger J, Sweasy JB. The I260Q Variant of DNA Polymerase β Extends Mispaired Primer Termini Due to Its Decreased Affinity for Deoxynucleotide Triphosphate Substrates. Biochemistry. 2008; 47:12118–12125. [PubMed: 18937502]

(26). Roettger MP, Bakhtina M, Tsai M-D. Mismatched and Matched dNTP Incorporation by DNA Polymerase β Proceed via Analogous Kinetic Pathways. Biochemistry. 2008; 47:9718–9727. [PubMed: 18717589]

(27). Dalal S, Kosa JL, Sweasy JB. The D246V mutant of DNA polymerase β misincorporates nucleotides: Evidence for a role for the flexible loop in DNA positioning within the active site. J. Biol. Chem. 2004; 279:577–584. [PubMed: 14563842]

(28). Shah AM, Li S-X, Anderson KS, Sweasy JB. Y265H Mutator Mutant of DNA Polymerase β. J. Biol. Chem. 2001; 276:10824–10831. [PubMed: 11154692]

(29). Iwanaga A, Ouchida M, Miyazaki K, Hori K, Mukai T. Functional mutation of DNA polymerase β found in human gastric cancer: Inability of the base excision repair in vitro. Mutat. Res. 1999; 435:121–128. [PubMed: 10556592]

(30). Lang T, Dalal S, Chikova A, DiMaio D, Sweasy JB. The E295K DNA Polymerase β Gastric Cancer-Associated Variant Interferes with Base Excision Repair and Induces Cellular Transformation. Mol. Cell. Biol. 2007; 27:5587–5596. [PubMed: 17526740]

(31). An CL, Chen D, Makridakis NM. Systematic Biochemical Analysis of Somatic Missense Mutations in DNA Polymerase β Found in Prostate Cancer Reveal Alteration of Enzymatic Function. Hum. Mutat. 2011; 32:415–423. [PubMed: 21305655]

(32). Tang K-H, Nieburh M, Tung C-S, Chan H.-c. Chou C-C, Tsai MD. Mismatched dNTP incorporation by DNA polymerase β does not proceed via globally different conformational pathways. Nucleic Acids Res. 2008; 36:2948–2957. [PubMed: 18385153]

(33). Starcevic D, Dalal S, Sweasy JB. Hinge Residue Ile260 of DNA Polymerase β is Important for Enzyme Activity and Fidelity. Biochemistry. 2005; 44:3775–3784. [PubMed: 15751954]

(34). Pelletier H, Sawaya MR, Kumar A, Wilson SH, Kraut H. Structure of Ternary Complexes of Rat DNA Polymerase β, a DNA Template-Primer, and ddCTP. Science. 1994; 264:1891–1903. [PubMed: 7516580]

(35). Lin GC, Jaeger J, Sweasy JB. Loop II of DNA polymerase β is important for polymerization activity and fidelity. Nucleic Acids Res. 2007; 35:2924–2935. [PubMed: 17439962]

(36). Kosa JL, Sweasy JB. 3′-Azido-3′-deoxythymidine-resistant Mutants of DNA Polymerase β Identified by *in Vivo* Selection. J. Biol. Chem. 1999; 274:3851–3858. [PubMed: 9920940]

(37). Joyce CM, Grindley ND. Construction of a plasmid that overproduces the large proteolytic fragment (Klenow fragment) of DNA polymerase I of *Escherichia coli*. Proc. Natl. Acad. Sci. U.S.A. 1983; 80:1830–1834. [PubMed: 6340110]

(38). Derbyshire V, Grindley NDF, Joyce CM. The 3′-5′ exonuclease of DNA polymerase I of *Escherichia coli*: Contribution of each amino acid at the active site to the reaction. EMBO J. 1991; 10:17–24. [PubMed: 1989882]

(39). Otwinowski Z, Minor W. Processing of X-ray diffraction data collected in oscillation mode. Methods Enzymol. 1997; 276:307–326.

(40). Battye TGG, Kontogiannis L, Johnson O, Powell HR, Leslie AGW. iMOSFLM: A new graphical interface for diffraction-image processing with MOSFLM. Acta Crystallogr. 2011; D67:271–278.

(41). Adams PD, Afonine PV, Bunkoczi G, Chen VB, Davis IW, Echols N, Headd JJ, Hung L-W, Kapral GJ, Grosse-Kunstleve RW, et al. PHENIX: A comprehensive Python-based system for macromolecular structure solution. Acta Crystallogr. 2010; D66:213–221.

(42). McCoy AJ, Grosse-Kunstleve RW, Adams PD, Winn MD, Storoni LC, Read RJ. Phaser crystallographic software. J. Appl. Crystallogr. 2007; 40:658–674. [PubMed: 19461840]

(43). Emsley P, Lohkamp B, Scott WG, Cowtan K. Features and development of Coot. Acta Crystallogr. 2010; D66:486–501.

(44). Kleywegt G. Use of non-crystallographic symmetry in protein structure refinement. Acta Crystallogr. 1996; D52:842–857.

(45). Davis IW, Leaver-Fay A, Chen VB, Block JN, Kapral GJ, Wang X, Murray LW, Arendall WB, Snoeyink J, Richardson JS, et al. MolProbity: All-atom contacts and structure validation for proteins and nucleic acids. Nucleic Acids Res. 2007; 35:W375–W383. [PubMed: 17452350]

(46). DeLano, WL. PyMol. DeLano Scientific; San Carlos, CA: 2001.

(47). Dalal S, Chikova A, Jaeger J, Sweasy JB. The Leu22Pro tumor-associated variant of DNA polymerase β is dRP lyase deficient. Nucleic Acids Res. 2008; 36:411–422. [PubMed: 18039710]

(48). Sawaya MR, Pelletier H, Kumar A, Wilson SH, Kraut J. Crystal Structure of Rat DNA Polymerase β: Evidence for a Common Polymerase Mechanism. Science. 1994; 264:1930–1935. [PubMed: 7516581]

(49). Arndt JW, Gong W, Zhong X, Showalter AK, Liu J, Dunlap CA, Lin Z, Paxson C, Tsai M-D, Chan MK. Insight into the Catalytic Mechanism of DNA Polymerase β: Structures of Intermediate Complexes. Biochemistry. 2001; 40:5368–5375. [PubMed: 11330999]

(50). Batra VK, Beard WA, Shock DD, Krahn JM, Pedersen LC, Wilson SH. Magnesium-Induced Assembly of a Complete DNA Polymerase Catalytic Complex. Structure. 2006; 14:757–766. [PubMed: 16615916]

(51). Pelletier H, Sawaya MR, Wolfle W, Wilson SH, Kraut J. Crystal Structures of Human DNA Polymerase β Complexed with DNA: Implications for Catalytic Mechanism, Processivity, and Fidelity. Biochemistry. 1996; 35:12742–12761. [PubMed: 8841118]

(52). Beard WA, Prasad R, Wilson SH. Activities and mechanism of DNA polymerase β. Methods Enzymol. 2006; 408:91–107. [PubMed: 16793365]

(53). Beard WA, Osheroff WP, Prasad R, Sawaya MR, Jaju M, Wood TG, Kraut J, Kunkel TA, Wilson SH. Enzyme-DNA Interactions Required for Efficient Nucleotide Incorporation and Discrimination in Human DNA Polymerase β. J. Biol. Chem. 1996; 271:12141–12144. [PubMed: 8647805]

(54). Kunkel TA. The Mutational Specificity of DNA Polymerase-β during in Vitro DNA Synthesis. J. Biol. Chem. 1985; 260:5787–5796. [PubMed: 3988773]

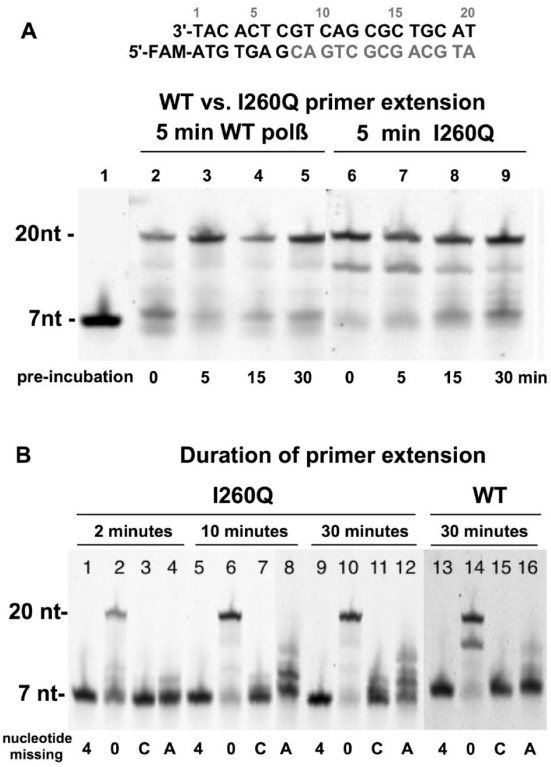

Figure 1.

In vitro primer extension assays on short dsDNA used for cocrystallization. (A) The activity of I260Q and wild type pol β was tested by using a 5′-FAM-labeled primer, otherwise of the same composition as that used in cocrystallization studies. The polymerase–DNA complexes, at a 10:1 ratio, were incubated at 37 °C (times of preincubation indicated below lanes) prior to the addition of $MgCl_2$ and dNTPs. Samples were separated on a 15% TBE-urea denaturing PAGE gel after primer extension for 5 min. The unextended substrate (7 nucleotides) and the fully extended product (20 nucleotides) are labeled at the left. Lane 1 contained the primer alone (the negative control). Unlike wild type pol β, I260Q is more adept at extending the primer, even without preincubating the reaction mix (lane 2 vs lane 6). This is evident by the amount of unextended primer remaining in lanes 2 and 6 (equivalent to 7 nucleotides) relative to the amount of fully extended primer (equivalent to 20 nucleotides). See Experimental Procedures for further experimental details. (B) Activity of wild type vs I260Q mutator pol β in the absence of dCTP or dATP, the first or second nucleotide required for primer extension, respectively. The polymerase–DNA complexes, at a 10:1 ratio, were preincubated for 5 min, after which dNTPs and $MgCl_2$ were added. Positive (all four dNTPs) and negative (sans dNTPs and $MgCl_2$) controls are indicated by "4" and "0" missing nucleotides below the respective lanes. The mutator exhibits extension in the absence of dATP after just 2 min (lane 4) and after 30 min in the absence of dCTP (lane 11).

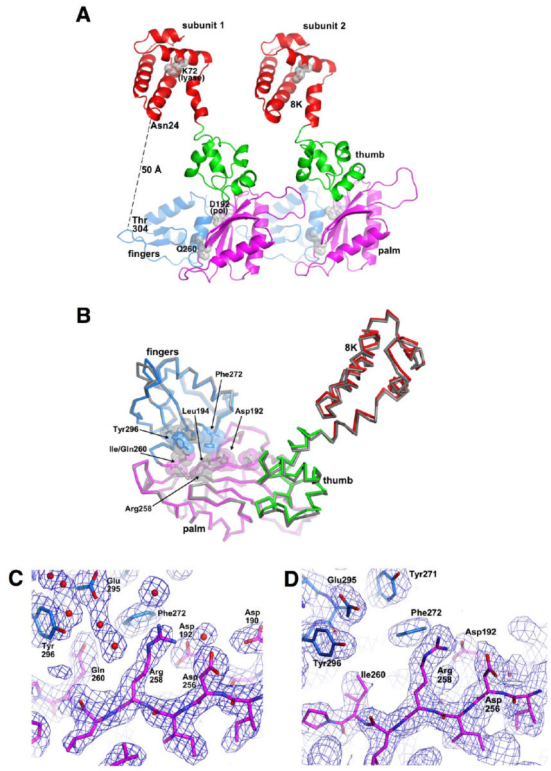

Figure 2.

Structure of apoenzyme I260Q pol β. (A) The asymmetric unit of this new monoclinic crystal form ($P2_1$) contains two pol β molecules related by a translation of 36 Å approximately along a. Both molecules adopt a wide-open conformation not observed before. The distance between the N-terminal subdomain (Asn24 on helix A) and the tip of the fingers subdomain (residue Thr304) is ~50 Å. (B) Comparison of I260Q and wild type apoenzyme pol β. The mutant is shown in subdomain colors (8 kDa, red; thumb, green; palm, magenta; fingers, blue), and the wild type structure is colored gray. Overall, the apoenzyme polymerase structures superimpose well. The amino acids near residue 260, namely, Asp192, Leu194 (obstructed), Arg258, Phe272, and Tyr296, relative positions indicated with arrows, show only minor shifts. (C) Water molecules, illustrated as red spheres, enter the hydrophobic hinge region in I260Q apoenzyme pol β. The electron density maps of both I260Q molecules A (and B, not depicted) consistently show water molecules entering the hinge region between the side chains of Gln260, Tyr296, and Arg258. (D) Water molecules are not observed in the corresponding areas of the wild type electron density maps.

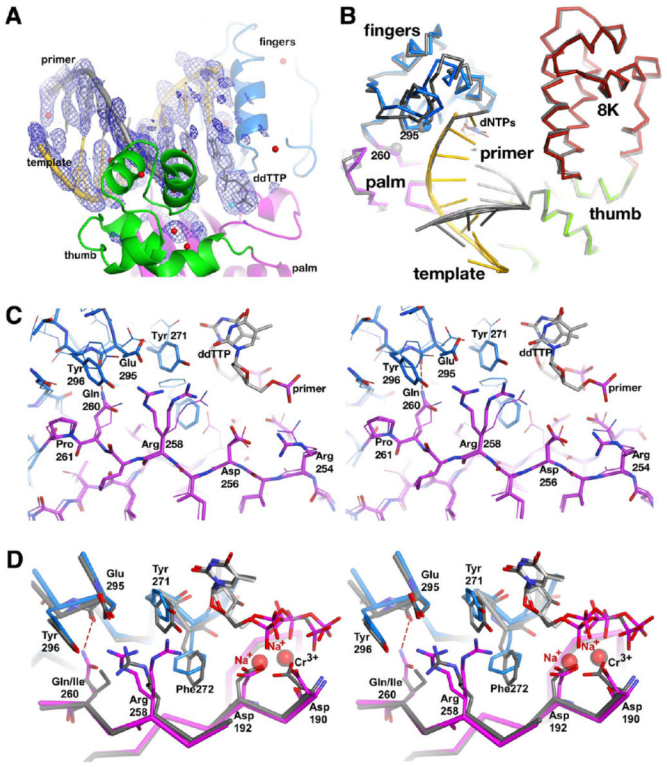

Figure 3.

I260Q ternary complex with dsDNA and ddTTP. (A) Omit electron density map showing dsDNA and ddTTP bound at the polymerase active site. The bias-free electron density "kick" map was calculated in PHENIX by omitting the substrate atoms from the Fourier calculations and by adding small random motions to the remaining protein atoms. The density map is contoured at 2.5 rmsd above the mean density in the ASU. The protein is shown in subdomain colors (see Figure 2B for definitions), and the primer and template are colored silver and gold, respectively. (B) Superposition of the ternary complexes of I260Q and the wild type (PDB entry 1HUO). The color coding for I260Q is as described above, whereas the wild type pol β backbone trace is colored gray. The α-carbon positions of Gln260 and Glu295 are labeled and highlighted by small spheres. Note that helix N (residues 275–290) and the following loop region (residues 299–310) in the I260Q fingers domain have moved closer to the template strand compared to those in the wild type complex (PDB entry 1HUO). (C) Close-up view (wall-eyed stereoview) of the structural rearrangements near the site of mutation (I260Q). The red dashed line highlights the hydrogen bond between ND2 of Gln260 and the backbone oxygen of Glu295. There are also some close interactions of Asp192 and Arg258 in the apoenzyme structure (thin sticks). In the ternary complex (thick sticks), Asp192 has rotated into the active site to interact with the metal ions. Arg258 shows alternate side chain conformations. One alternate conformation (70% occupancy) forms hydrogen bonds with Glu295 (red dashes). (D) Comparison of the relevant active site region in the I260Q and wild type pol β ternary complexes in a wall-eyed stereoview. The color coding for I260Q is as described above, while the wild type pol β backbone trace is colored gray. The hydrogen bond (red dashes) between the Gln260 and Glu295 main chain, which is absent in the wild type pol β structure, further stabilizes the closed conformation of the I260Q mutator. The metal ions are shown as transparent spheres (Na^+, red; Cr^{3+}, gray). Metal ions B adjacent to the triphosphate group overlap completely.

Table 1

Crystallographic Data of DNA Polymerase β

	wild type-apo	**I260Q-apo**	**I260Q·dsDNA·ddTTP**
	Data Collection[a]		
a (Å)	77.86	77.9	100
b (Å)	67.83	67.35	56
c (Å)	83.29	82.37	93
β (deg)	116.07	115.74	102
resolution range (Å)	25.0–2.5 (2.58–2.5)	24.0–2.0 (2.14–2.1)	27.2–2.72 (2.8–2.75)
R_{merge} (%)[b]	10 (56.8)	9.2 (51.6)	6.3 (52.7)
completeness (%)	89.6 (87.0)	93.77 (81)	90.1 (66)
$I/\sigma I$	12.45 (1.8)	12.8 (2.0)	18.75 (1.6)
no. of reflections			
observed	64617	175067	196834
unique	24378	36809	25065
	Refinement		
rmsd			
bond lengths (Å)	0.009	0.008	0.009
bond angles (deg)	1.271	1.119	1.479
R_{work} (%)	25.01	23.90	21.82
R_{free} (%)	31.66	29.52	29.20
residue content			
amino acids	650	650	656
waters	159	281	47
PDB entry	3UXN	3UXO	3UXP

[a] Values in parentheses refer to those of the highest-resolution shell.

[b] $R_{\text{merge}} = 100\Sigma_h\Sigma_i|I_{h,i} - I_h|/\Sigma_h\Sigma_i I_{h,i}$, where I_h is the mean intensity of symmetry-related reflections, $I_{h,i}$.